Data quantification

The same dendritic segments (~5–20 μm in length; see Figs 2 and 3) were identified from three-dimensional image stacks taken from both views with high image quality (ratio of signal to background noise >4:1). These randomly chosen segments are probably mostly from different parent cells because of the high density of labelled neurons (>33 cells per 6,000 μm^2). The number and location of dendritic protrusions (protrusion length was more than one-third of dendritic shaft diameter) were identified in each view without prior knowledge of the animal's age, the interval between views or the order of the views. The total number of spines (N) was pooled from dendritic segments of different animals. Data throughout the text are presented as means ± s.d.

Filopodia were identified as long thin structures (generally larger than twice the average spine length, ratio of head diameter to neck diameter <1.2:1 and ratio of length to neck diameter >3:1). The remaining protrusions were classified as spines. Three-dimensional stacks were used to ensure that tissue movements and rotation between imaging intervals did not influence spine identification. Spines or filopodia were considered the same between two views on the basis of their spatial relationship to adjacent landmarks and their relative position to immediately adjacent spines (Figs 2 and 3). Spines in the second view were considered different if they were more than 0.7 μm from their expected positions based on the first view.

We chose 0.7 μm as a cut-off distance because apparent spine position can shift by up to ~0.3 μm in either direction along the axis of dendritic shafts owing to changes in spine morphology, slight tissue rotation and movements related to brain pulsation. We estimate the imaging resolution of our two-photon microscope (60 ×, numerical aperture 0.9, at 920 nm) to be ~0.7 μm. We found no significant changes in adult spine stability with three different cut-off distances (0.5, 0.7 and 0.9 μm), showing that our conclusion of spine stability is not dependent on minor changes in these criteria. Even though slight rotations of shafts and protrusions could either obscure existing spines (suggesting spine elimination) or reveal previously hidden spines (suggesting spine addition), such rotational artefacts would only underestimate the amount of stability observed.

For quantification of changes in spine morphology, we minimized the possibility of rotational artefacts by preselecting from three-dimensional image stacks only spines parallel to the imaging plane in both views. Dendrites containing saturated pixels were excluded. Imaging software (NIH ImageJ) was used to measure the spine length and head diameter of identical spines between views. The edges of spines were detected with a Sobel detector algorithm (ImageJ).

Curve fitting was done with the user-defined fitting function on Igor Pro (WaveMetrics, Lake Oswego, Oregon, USA). The single-exponential function was fitted to the data by using the built-in iterative Levenberg–Marquardt function to minimize χ^2.

Received 28 August; accepted 4 November 2002; doi:10.1038/nature01276.

1. Hubel, D. H., Wiesel, T. N. & LeVay, S. Plasticity of ocular dominance columns in monkey striate cortex. *Phil. Trans. R. Soc. Lond. B* **278,** 377–409 (1977).
2. Rakic, P., Bourgeois, J. P. & Goldman-Rakic, P. S. Synaptic development of the cerebral cortex: implications for learning, memory, and mental illness. *Prog. Brain Res.* **102,** 227–243 (1994).
3. Lichtman, J. W. & Colman, H. Synapse elimination and indelible memory. *Neuron* **25,** 269–278 (2000).
4. Buonomano, D. V. & Merzenich, M. M. Cortical plasticity: from synapses to maps. *Annu. Rev. Neurosci.* **21,** 149–186 (1998).
5. Florence, S. L., Taub, H. B. & Kaas, J. H. Large-scale sprouting of cortical connections after peripheral injury in adult macaque monkeys. *Science* **6,** 1117–1121 (1998).
6. Jones, E. G. & Pons, T. P. Thalamic and brainstem contributions to large-scale plasticity of primate somatosensory cortex. *Science* **282,** 1121–1125 (1998).
7. Lund, J. S., Boothe, R. G. & Lund, R. D. Development of neurons in the visual cortex (area 17) of the monkey (*Macaca nemestrina*): a Golgi study from fetal day 127 to postnatal maturity. *J. Comp. Neurol.* **176,** 149–188 (1977).
8. Rakic, P., Bourgeois, J. P., Eckenhoff, M. F., Zecevic, N. & Goldman-Rakic, P. S. Concurrent overproduction of synapses in diverse regions of the primate cerebral cortex. *Science* **11,** 232–235 (1986).
9. Shatz, C. J. & Stryker, M. P. Ocular dominance in layer IV of the cat's visual cortex and the effects of monocular deprivation. *J. Physiol. (Lond.)* **281,** 267–283 (1978).
10. Antonini, A., Fagiolini, M. & Stryker, M. P. Anatomical correlates of functional plasticity in mouse visual cortex. *J. Neurosci.* **1,** 4388–4406 (1999).
11. Bao, S., Chan, V. T. & Merzenich, M. M. Cortical remodelling induced by activity of ventral tegmental dopamine neurons. *Nature* **412,** 79–83 (2001).
12. Kleim, J. A. *et al.* Selective synaptic plasticity within the cerebellar cortex following complex motor skill learning. *Neurobiol. Learn. Mem.* **69,** 274–289 (1998).
13. Knott, G. W., Quairiaux, C., Genoud, C. & Welker, E. Formation of dendritic spines with GABAergic synapses induced by whisker stimulation in adult mice. *Neuron* **34,** 265–273 (2002).
14. Feng, G. *et al.* Imaging neuronal subsets in transgenic mice expressing multiple spectral variants of GFP. *Neuron* **28,** 41–51 (2000).
15. Fiala, J. C., Feinberg, M., Popov, V. & Harris, K. M. Synaptogenesis via dendritic filopodia in developing hippocampal area CA1. *J. Neurosci.* **18,** 8900–8911 (1998).
16. Dunaevsky, A., Blazeski, R., Yuste, R. & Mason, C. Spine motility with synaptic contact. *Nature Neurosci.* **4,** 685–686 (2001).
17. Dailey, M. E. & Smith, S. J. The dynamics of dendritic structure in developing hippocampal slices. *J. Neurosci.* **16,** 2983–2994 (1996).
18. Ziv, N. E. & Smith, S. J. Evidence for a role of dendritic filopodia in synaptogenesis and spine formation. *Neuron* **17,** 91–102 (1996).
19. Dunaevsky, A., Tashiro, A., Majewska, A., Mason, C. & Yuste, R. Developmental regulation of spine motility in the mammalian central nervous system. *Proc. Natl Acad. Sci. USA* **96,** 13438–13443 (1999).
20. Lendvai, B., Stern, E. A., Chen, B. & Svoboda, K. Experience-dependent plasticity of dendritic spines in the developing rat barrel cortex *in vivo*. *Nature* **404,** 876–881 (2000).
21. Boothe, R. G., Greenough, W. T., Lund, J. S. & Wrege, K. A quantitative investigation of spine and dendrite development of neurons in visual cortex (area 17) of *Macaca nemestrina* monkeys. *J. Comp. Neurol.* **186,** 473–489 (1979).
22. Huttenlocher, P. R. & de Courten, C. The development of synapses in striate cortex of man. *Hum. Neurobiol.* **6,** 1–9 (1987).
23. Bourgeois, J. P., Goldman-Rakic, P. S. & Rakic, P. Synaptogenesis in the prefrontal cortex of rhesus monkeys. *Cereb. Cortex* **4,** 78–96 (1994).
24. Harris, K. M. & Stevens, J. K. Dendritic spines of CA 1 pyramidal cells in the rat hippocampus: serial electron microscopy with reference to their biophysical characteristics. *J. Neurosci.* **9,** 2982–2997 (1989).
25. Murthy, V. N., Schikorski, T., Stevens, C. F. & Zhu, Y. Inactivity produces increases in neurotransmitter release and synapse size. *Neuron* **32,** 673–682 (2001).
26. Purves, D. & Hadley, R. D. Changes in the dendritic branching of adult mammalian neurones revealed by repeated imaging *in situ*. *Nature* **315,** 404–406 (1985).
27. Purves, D., Voyvodic, J. T., Magrassi, L. & Yawo, H. Nerve terminal remodeling visualized in living mice by repeated examination of the same neuron. *Science* **238,** 1122–1126 (1987).
28. Lichtman, J. W., Magrassi, L. & Purves, D. Visualization of neuromuscular junctions over periods of several months in living mice. *J. Neurosci.* **7,** 1215–1222 (1987).
29. Majewska, A., Yiu, G. & Yuste, R. A custom-made two-photon microscope and deconvolution system. *Pflügers Arch. Eur. J. Physiol.* **441,** 398–408 (2000).

Supplementary Information accompanies the paper on *Nature*'s website (http://www.nature.com/nature).

Acknowledgements We thank J. Lichtman, S. Burden and R. Yuste for critical comments on this manuscript. This work was supported by grants from the National Institutes of Health and the Ellison Foundation to W.-B.G. and by an Irene Diamond grant to M. L. Dustin for purchasing the imaging system.

Competing interests statement The authors declare that they have no competing financial interests.

Correspondence and requests for materials should be addressed to W.-B.G. (e-mail: gan@saturn.med.nyu.edu).

A role for casein kinase 2α in the *Drosophila* circadian clock

Jui-Ming Lin*†, Valerie L. Kilman*†, Kevin Keegan*, Brie Paddock*, Myai Emery-Le‡, Michael Rosbash‡ & Ravi Allada*§

** Department of Neurobiology and Physiology, and § Department of Pathology, Northwestern University, Evanston, Illinois 60208, USA*
‡ Howard Hughes Medical Institute, Brandeis University, Waltham, Massachusetts 02454, USA
† These authors contributed equally to this work

Circadian clocks drive rhythmic behaviour in animals and are regulated by transcriptional feedback loops[1,2]. For example, the *Drosophila* proteins Clock (Clk) and Cycle (Cyc) activate transcription of *period* (*per*) and *timeless* (*tim*). Per and Tim then associate, translocate to the nucleus, and repress the activity of Clk and Cyc. However, post-translational modifications are also critical to proper timing. Per and Tim undergo rhythmic changes in phosphorylation[1], and evidence supports roles for two kinases in this process: Doubletime (Dbt) phosphorylates Per[3,4], whereas Shaggy (Sgg) phosphorylates Tim[5]. Yet Sgg and Dbt often require a phosphoserine in their target site[6,7], and analysis of Per phosphorylation in *dbt* mutants[3,8] suggests a role for other kinases. Here we show that the catalytic subunit of *Drosophila* casein kinase 2 (CK2α) is expressed predominantly in the cytoplasm of key circadian pacemaker neurons. *CK2α* mutant flies show lengthened circadian period, decreased CK2 activity, and delayed nuclear entry of Per. These effects are probably direct, as CK2α specifically phosphorylates Per *in vitro*. We propose that CK2 is an evolutionary link between the divergent circadian systems of animals, plants and fungi.

To identify new components of circadian clocks, we screened

about 2,000 ethylmethane-sulphonate (EMS)-mutagenized *per*^{s} (short-period allele of *per*) lines for circadian behavioural defects. A dominant mutant, *Timekeeper (Tik)*, was identified. *Tik* homozygotes do not live to adulthood. *Tik* heterozygotes exhibited behavioural rhythms approximately 1.5 h longer than *per*^{s} (Table 1). In a *per*$^{+}$ or *per*^{l} (long-period allele of *per*) background, *Tik* lengthened the period of the behavioural rhythm by 3 h, reflecting an allele-specific interaction between *per* and *Tik* (Table 1). During our studies, we identified a spontaneous partial revertant, *TikR* (Table 1), and we could not separate this revertant from *Tik* by recombination (0 out of 77 recombinants). *TikR* retains the flanking *Tik* markers, *roughoid*, *rosy* and *spineless*, and fails to complement the recessive lethality of *Tik*. The change in period in *Tik* mutants (about 3 h) exceeds that of nearly all heterozygous circadian mutants in *Drosophila*, suggesting that it might identify a protein of central importance in the circadian clock mechanism.

Using standard meiotic mapping and male recombination[9], we mapped *Tik* to a region around the centromere of chromosome 3 (Table 2; see also Methods). We were unable to identify homozygous-viable *Tik* recombinants, nor do these recombinants complement each other for lethality, suggesting that *Tik* is a vital gene. We searched the non-recombinant interval for candidate genes, and initially focused on a candidate serine-threonine kinase, the catalytic α-subunit of casein kinase 2 (*CK2α*)[10]. Sequencing of the *CK2α* coding region from the wild-type parental strain and the initial *Tik* mutant identified two sequence changes, both resulting in coding changes: Met161Lys and Glu165Asp. The change from the non-charged Met 161 to the charged Lys occurs near the catalytic loop and within a hydrophobic binding pocket for ATP[11]. We also sequenced the *TikR* mutant that we proposed was a new *Tik* revertant allele. In addition to the two original *Tik* coding changes, we identified an additional in-frame, 27-base-pair (bp) deletion coupled to an in-frame, 6-bp insertion, resulting in a deletion of 7 amino acids (234–240) and another amino acid change (Arg242-Glu). These mutations occur in residues that are highly conserved with their human counterpart.

To confirm that the observed mutations were functional, we established a biochemical assay of CK2 activity[12]. CK2 was immunoprecipitated from adult head extracts using an antibody that recognizes the CK2 holoenzyme (two catalytic α- and two regulatory β-subunits)[13]. To verify that immunoprecipitated kinase activity was due to CK2, we measured the activity in the presence of heparin, a specific CK2 inhibitor. We found that 5 μg ml^{-1} heparin was able to reduce the activity of immunoprecipitated CK2 by about 90%, comparable to that of heparin against purified rat CK2 (data not shown). We did not observe any significant change in CK2 activity as a function of time in a 12-h light/dark cycle (Fig. 1a). We then measured CK2 activity in *CK2α*^{Tik} and *CK2α*^{TikR} heterozygotes. We found activity reductions in the *CK2α*^{Tik} heterozygotes and a return to near wild-type levels in *CK2α*^{TikR} (Fig. 1b). These *in vivo* biochemical measurements demonstrate that a loss (and its partial reversion) of CK2 enzymatic function is strongly correlated with changes in circadian period. Thus, the effects on the circadian

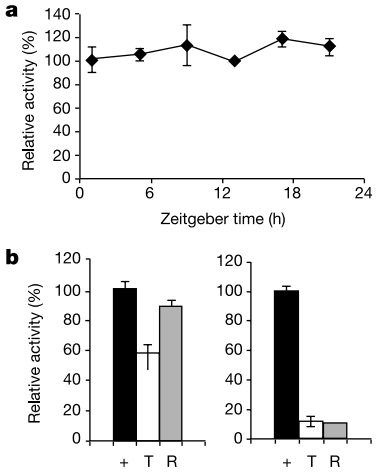

Figure 1 Biochemical activity of wild-type and mutant CK2α. **a**, Diurnal regulation of CK2 activity. The graph displays the average of two experiments with ZT 13 set to 100. **b**, CK2 activity immunoprecipitated from head extracts (left panel). +, wild type; T, *Tik*/ + ; R, *TikR*/ + . The graph shows the average of three experiments in duplicate with wild-type set to 100%. Error bars indicate standard error of the mean (s.e.m.). $P = 0.0003$ for wild type compared with *Tik*/ + ; $P = 0.003$ for *Tik*/ + compared with *TikR*/ + . The right panel shows recombinant CK2α activity. Wild-type (+) is normalized to 100. Error bars indicate s.e.m. from six measurements (three experiments; $P < 0.00002$ for wild-type compared with *Tik*/ +). Owing to the difficulty of obtaining material, TikR (R) activity was determined from one experiment.

cycle associated with the *CK2α*^{Tik} allele are probably due to a loss of CK2 function and not another effect of the mutation.

To determine clearly their biochemical defects, we assayed the activity of bacterially expressed wild-type and mutant CK2α. We found that the recombinant CK2α^{Tik} mutant subunit was substantially less active than the wild type (Fig. 1b). We also found that the CK2α^{TikR} mutant had comparable catalytic activity to CK2α^{Tik}, suggesting that the reversion does not alter catalytic activity relative to CK2α^{Tik}. Notably, the CK2α^{TikR} protein was much less soluble, suggesting that folding of CK2α^{TikR} is altered *in vivo*, thus blocking incorporation into the CK2 holoenzyme. As a result, the CK2 holoenzyme in *CK2α*^{TikR} heterozygotes would consist largely of wild-type α-subunits. In this case, the period change (about 1 h) observed in these flies would be due to a reduction of wild-type gene dosage. Consistent with this hypothesis, homozygous *TikR* flies are not adult-viable.

If CK2α is involved directly in circadian rhythms, it should be expressed in circadian pacemaker neurons. We performed immunohistochemistry on adult whole-mount dissected brains with an antiserum directed against a CK2 peptide sequence common to

Table 1 **Circadian locomotor activity in *Tik* mutants**

Genotype	Period (h) ± s.e.m.	Rhythmic (%)
+/+	23.6 ± 0.1	95 (43)
Tik/ +	26.4 ± 0.1	88 (32)
TikR/ +	24.3 ± 0.1	100 (24)
per^{s}; + /+	18.9 ± 0.1	100 (16)
per^{s};*Tik*/ +	20.4 ± 0.1	80 (15)
per^{l}	29.6 ± 0.1	100 (10)
per^{l};*Tik*/ +	32.5 ± 0.1	84 (7)

The number of flies analysed is indicated in parentheses in the final column. +, wild type; *Tik*, *Timekeeper*, *TikR*, *Timekeeper* revertant. Rhythmic (%) refers to the percentage of flies that were scored as rhythmic (see Methods). *per*^{s} and *per*^{l} are long and short period alleles of *period*.

Table 2 **Mapping of *Tik***

Marker	Recombinants	Map
cyc	4/459 (R)	76C
l(3)s2253	2/112 (R)	77A
ri	3/230 (R)	77E
Ten-m05309	1/142 (R)*	79E1–79E2
nrmA37	4/393 (R)*	80A1–80A2
Centromere	–	80F–81F
EP3028	1/1,233 (L)*	82A?
l(3)L1233	1/896 (L)*	82B1–82B2
Ki	4/88 (L)	83D

The recombinants column indicates the number of recombinants out of the total number that were screened. R and L in parentheses indicate that *Tik* maps to the right or left, respectively. The position of EP3028 was inferred from genomic location. *cyc*, *cycle*; *ri*, *radius incompletus*; *Ki*, *Kinked*.
*Male recombination.

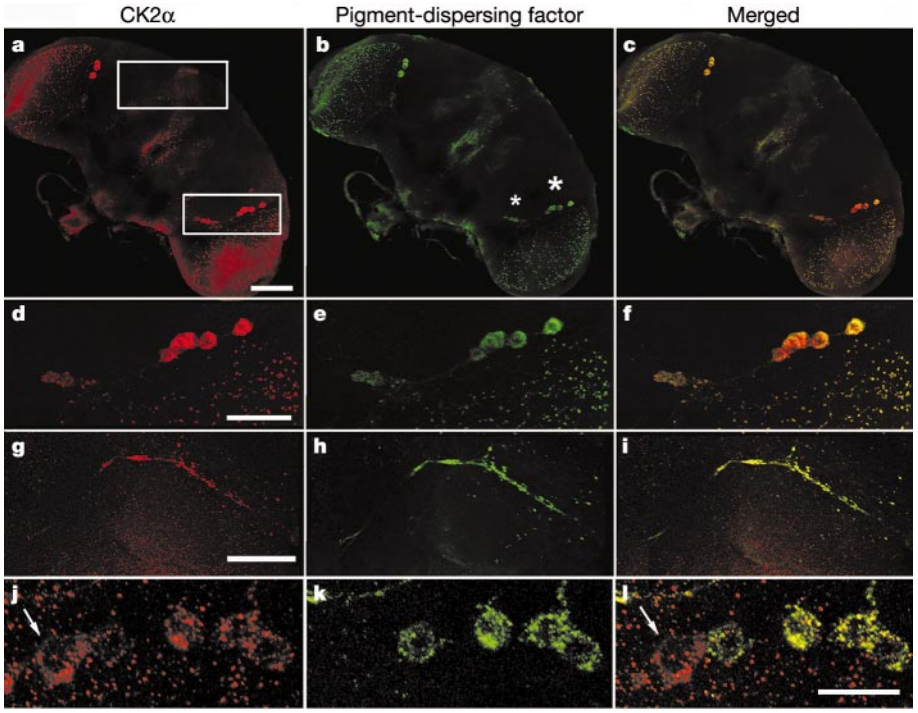

Figure 2 *Drosophila* CK2α is primarily expressed in circadian pacemaker cells. **a**–**i**, Immunofluorescence of adult brain stained for CK2α and Pigment-dispersing factor (Pdf) at ZT 18. The large and small asterisks indicate large and small lymph nodes, respectively. **d**–**f**, Magnified images of the lower boxed area in **a** showing lymph-node staining and punctate terminals of the large lymph nodes in the medulla. **g**–**i**, Magnified images of the upper boxed area in **a**. The posterior brain shows double-labelled projections of the small lymph node to the superior protocerebrum. Scale bars: **a**–**c**, 100 μm; **d**–**f**, 50 μm; **g**–**i**, 50 μm. **j**–**l**, Whole-mount immunofluorescence for CK2α and Pdf in third instar larval brain. The white arrows indicate a CK2α-positive but Pdf-negative cell body. Scale bar, 10 μm.

both fly and mammalian CK2α (anti-CK2α). Anti-CK2α specifically labels the cytoplasm and axonal projections of neurons in the lateral protocerebrum (Fig. 2a, d, g). To determine whether these neurons were the well-described pacemaker lateral neurons, we performed double labelling with an antiserum against Pigment-dispersing factor (Pdf)[14–16]. This neuropeptide is specifically localized to small and large lateral neurons critical to behavioural rhythms (Fig. 2b, e, h). Consistent with its proposed circadian role, CK2 co-localizes with Pdf in these adult neurons (Fig. 2c, f, i). The CK2 antiserum also variably labels two cells in the dorsal brain, but they are labelled much less intensely than the lateral neurons (data not shown). CK2α is also probably expressed in the eyes, as CK2 activity is modestly reduced (about 20%) in *eyes absent* mutants (data not shown). Of note, CK2α and Pdf also co-localize to neuronal termini, indicating that CK2 may regulate directly Pdf processing or release. CK2α seems to be constitutively cytoplasmic as a function of the time of day (data not shown). To confirm that anti-CK2α specifically recognizes CK2α, we performed single

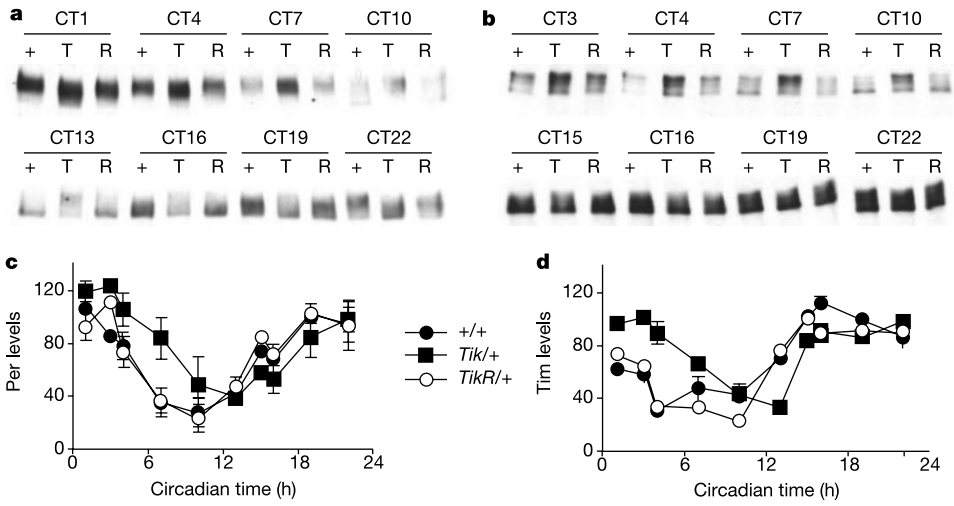

Figure 3 Circadian regulation of Per and Tim in *CK2α* mutants. **a**, Western blot of Per. CT indicates circadian time, where CT0 is 12 h after lights off. +, wild type; T, *Tik*; R, *TikR*. **b**, Western blot of Tim. **c**, **d**, Quantification of Per and Tim western blots. Each point is the average of two to three independent experiments except for CT3 and CT15 for both Per and Tim, and CT1 for Tim alone. Error bars indicate s.e.m.

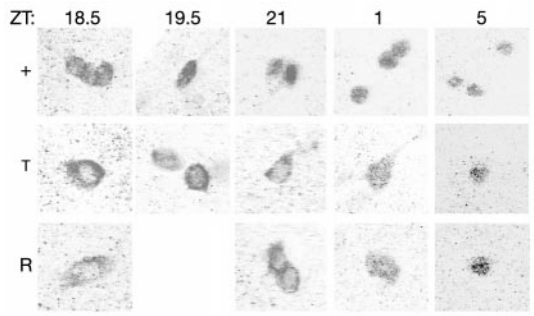

Figure 4 Nuclear entry of Per in homozygous *CK2α* mutants. +, wild type; T, *Tik/Tik* homozygotes; R, *TikR/TikR* homozygotes. Homozygous larvae were reared in a 12-h light/dark cycle. ZT, Zeitgeber time (ZT).

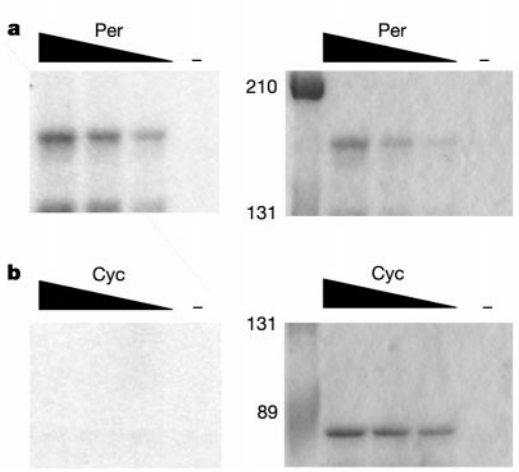

Figure 5 Phosphorylation by CK2α is period-specific. **a**, *In vitro* phosphorylation by CK2α of bacterially expressed and purified Per (left panel). The right panel shows Coomassie-stained Per as a loading control. Per varies from 0.125 to 0.5 μg. **b**, *In vitro* phosphorylation by CK2α of bacterially expressed and purified Cyc (left panel). The right panel shows Coomassie-stained Cyc as a loading control. Cyc varies from 0.25 to 0.5 μg. Numbers represent relative molecular mass ($\times 10^3$).

labelling with anti-CK2α alone and found a similarly specific expression pattern, which is specifically blocked by 10^{-6} M of recombinant CK2α but not by an unrelated antigen (data not shown). Western analysis confirmed this specificity. We also found that the CK2α antiserum labels a Pdf-negative cell in larval brains, indicating that the observed signal is not attributable to the Pdf signal (Fig. 2j–l). The tissue specificity of CK2α expression suggests that it has a specific function in circadian clocks.

To ascertain CK2 function on Per and Tim, we examined their levels and phosphorylation in heterozygotes. Flies were entrained in a light/dark cycle and were transferred to constant darkness (DD). During the early subjective day (circadian time, CT, 0–12) levels of Per in the $CK2\alpha^{Tik}$ mutants are increased and show delayed disappearance (Fig. 3a). Furthermore, there seems to be a modest increase in less-phosphorylated forms of Per. During the subjective night, Per phosphorylation and to a lesser extent accumulation are delayed relative to wild type. An increase in the level of Per and Tim in $CK2\alpha^{Tik}$ mutants is delayed by approximately 3 h relative to wild type, consistent with the period-lengthening effect of $CK2\alpha^{Tik}$ mutants (Fig. 3c and Table 1). Disappearance of Tim is also more strongly affected than accumulation in $CK2\alpha^{Tik}$ mutants (Fig. 3b, d). The Per and Tim profiles of $CK2\alpha^{TikR}$ heterozygotes are largely unchanged, consistent with its heterozygous behavioural and biochemical phenotypes.

To examine the phenotype of homozygous CK2α mutants, we performed immunofluorescence for Per in third-instar larval brains. Consistent with previous studies we found that Per staining in wild-type larvae is predominantly nuclear by Zeitgeber time (ZT) 21 (Fig. 4). In $CK2\alpha^{Tik}$ and $CK2\alpha^{TikR}$ homozygotes, however, Per nuclear entry is significantly delayed, with Per predominantly cytoplasmic at ZT21. By ZT1, the Per staining pattern in the *CK2α* mutants remains distinct from the wild-type nuclear pattern, appearing to be present in both cytoplasmic and nuclear compartments. These data demonstrate a strong effect of CK2α on Per nuclear entry and are consistent with the cytoplasmic expression of CK2α. Furthermore, we did not observe significant differences between $CK2\alpha^{Tik}$ and $CK2\alpha^{TikR}$, consistent with biochemical data on recombinant proteins (Fig. 3b) and their recessive lethality. These data support our model that $CK2\alpha^{TikR}$ is a strong loss-of-function allele, lacking the strong dominant behavioural and biochemical effects of $CK2\alpha^{Tik}$.

Previous studies have shown that CK2 phosphorylates Per and Tim *in vitro*, suggesting direct effects of CK2 (ref. 17). Consistent with previous reports, we found that bacterially expressed and purified CK2α can phosphorylate Per *in vitro* (Fig. 5a). Notably, this effect is specific, as we do not observe significant phosphorylation of the circadian transcription factor Cyc. We also found that Tim (amino acids 1–1159) is phosphorylated by CK2α to a lesser extent than Per (data not shown). These data are consistent with the direct regulation of Per and Tim by CK2.

Taken together, our analysis indicates a dedicated and direct role of CK2 in the *Drosophila* circadian clock mechanism. $CK2\alpha^{Tik}$ has one of the strongest phenotypes of any heterozygous circadian rhythm mutant. The modest nature of the biochemical defect further supports the hypothesis that the circadian clock is highly sensitive to CK2 activity. The CK2α expression pattern (Fig. 2) indicates that it has a specific role in circadian rhythms. Its localization to neuronal termini raises the possibility that CK2 links the clock to circadian outputs.

We favour the model that CK2 directly phosphorylates Per and Tim *in vivo*, promoting their transition to the nucleus. The evidence for this pattern is compelling for Per. Allele-specific interactions between *per* and *CK2α* alleles support the model of a direct interaction. It has been shown that CK2 can phosphorylate both Per and Tim *in vitro*[17]. By comparison with protein kinases A and C, CK2 is much more specific, as demonstrated by the paucity of other ^{32}P-labelled proteins in the immunoprecipitate[17]. We have also shown that CK2 can specifically phosphorylate Per *in vitro* (Fig. 5). Given the cytoplasmic expression of CK2α, this phosphorylation may serve as a signal for nuclear entry and subsequent degradation, explaining the delayed nuclear entry and disappearance of these proteins in $CK2\alpha^{Tik}$ mutants.

This study also establishes an evolutionary connection between animal, plant and fungal circadian systems—genetic studies have revealed clock components in plants (*Arabidopsis*) and fungi (*Neurospora*). These studies suggest that clocks have arisen several times in evolution[18]; however, studies in both *Arabidopsis* and *Neurospora* have linked CK2 to circadian timekeeping[19–21]. *CK2* is therefore a gene involved in circadian rhythms that is shared between all three phylogenetic kingdoms. Indeed, the fly enzyme (amino acids 7–322) shares 77% and 72% identity with the *Arabidopsis* and *Neurospora* enzymes, respectively. We propose that the conserved role for CK2 is driven by the need to avoid mutagenic ultraviolet light. CK2 has a pivotal role in the response to ultraviolet radiation from yeast to humans[22,23]. Consistent with this model, cryptochromes, components of plant and animal circadian systems, are homologous to ultraviolet-dependent DNA repair enzymes[24]. Given this strong conservation, the circadian role of mammalian CK2α

homologues should be of great interest.

Note added in proof: Recent work from F. R. Jackson and others demonstrates a role for the β-subunit of CK2 in *Drosophila* circadian rhythms. □

Methods

Drosophila genetics

per^{s}; *ry*^{506} flies were used for mutagenesis and as controls for identifying mutations[25]. Fly stocks are from Bloomington Stock Center. Initial mapping with *roughoid* (*ru*), *spineless* (*ss*) and *claret* (*ca*) identified approximately 10% recombination between *ry*^{506} and *Tik*. Scoring of flanking markers indicated that *Tik* mapped to the left of *ry*. Further mapping of informative recombinants is summarized in Table 2. Uninformative meiotic recombination experiments are as follows: Y257 (79C; 0 out of 313), l(3)L7251 (79F; 0 out of 211), l(3)J1E6 (82A; 0 out of 111). We were unable to find deficiencies that failed to complement the circadian or lethal phenotypes.

Circadian locomotor activity analysis

Flies were entrained for 2–5 days in 12-h light/dark conditions, and locomotor activity behaviour was monitored subsequently in constant darkness for 6–8 days as described previously using Trikinetics locomotor activity monitors[26]. We performed χ^2 periodogram analysis ($\alpha = 0.01$) of locomotor activity using the ClockLab software package (Actimetrics). Flies whose χ^2 statistic exceeded the significance line by 5 were judged to be significantly rhythmic, and were used for period calculations.

Bacterial expression and recombinant protein purification

Wild-type and mutant *CK2α* coding regions were amplified (Pfu turbo; Stratagene) from genomic DNA, subcloned into pET-30(a), expressed in BL21, and purified using His and S tags (Novagen). We confirmed the presence or absence of mutations by sequencing. Per was amplified by polymerase chain reaction (PCR) (Pfu turbo; Stratagene), subcloned into pQE-80L (Qiagen), expressed in DH5α, and purified using a His tag, following the manufacturer's instructions. His-tagged Per adds a further 32 amino acids to the amino-terminus, which does not contain any consensus CK2 sites. Per phosphorylation results were confirmed by testing two independent clones. Expression of glutathione *S*-transferase (GST)–Tim(1–1159) and GST–Cyc (also known as dBmal) was performed as in ref. 5.

CK2 activity assays

Fly head extracts were prepared[8] and normalized to the same protein concentration by Bradford assay. Immunoprecipitation was performed[17] with a CK2 antibody that recognizes the *Drosophila* holoenzyme (anti-CK2H)[13], with the following changes: 40 μl beads, 500 μl extraction buffer washes, 0.5 μl anti-CK2, and 150 μl of extract was added (5–8 mg ml^{-1}). The mixture was incubated end-over-end for 4 h. Beads were washed twice for 5 min then once with 500 μl CK2 assay buffer (50 mM Tris, pH 8.5, 100 mM NaCl, 10 mM $MgCl_2$). Beads were then incubated with 25 μl CKII activity assay buffer, 1 mg ml^{-1} biotinylated peptide containing an optimized CK2 target site, [biotin]-RRREEETEEE-[OH] (Princeton BioMolecules), 0.1 mM ATP, 0.6 μl [γ-^{32}P]ATP. This reaction was incubated end-over-end at room temperature for 10 min. For recombinant CK2α, 25 μl CK2 assay buffer (50 mM Tris, pH 8.5, 100 mM NaCl, 10 mM $MgCl_2$, 1 mg ml^{-1} biotinylated peptide, 1.5 μl [γ-^{32}P]ATP) was incubated for 30 min at room temperature with 2.5 μg recombinant protein. We added 15 μl of 7.5 M guanidine-HCl to stop the reaction. A total of 25 μl supernatant from the reaction was transferred to a SAM^2 biotin-capture membrane (Promega) until dry. Each membrane was washed individually using a 6-well culture plate at room temperature as follows: 5 ml of 1 M NaCl four times for 1 min; 5 ml of 1 M NaCl with 1% phosphoric acid twice for 1 min; 5 ml of water once for 1 min; and 95% alcohol once for 15 s.

For Per, Tim and Cyc *in vitro* kinase reactions, 100 μl CK2 kinase assay buffer (50 mM Tris, pH 8.5, 100 mM NaCl, 10 mM $MgCl_2$, 0.5 μl [γ-^{32}P]ATP) containing recombinant protein was incubated at room temperature for 10 min. We used 0.2 μg CK2α for each assay, and we used 0.1–0.5 μg of Per and Cyc. After the kinase reaction, the proteins were precipitated by tricarboxylic acid to remove free nucleotide, and boiled in × 2 SDS gel loading buffer.

Immunohistochemistry

Adult and larval brains were fixed and stained for whole-mount immunofluorescence[27] with the following exceptions: 10% donkey normal serum and no bovine serum albumin were used for blocking and antibody incubations, primary antibody incubations were ≥24 h, and only secondary (not tertiary) antibodies were used. Affinity purified antibodies were diluted to 1.7–8.5 μg ml^{-1} (rabbit anti-CK2α (StressGen); 1:100–200 rat anti-Pdf[28], 1:100–300 Cy3-labelled donkey anti-rabbit, and/or 1:100–300 fluorescein isothiocyanate-donkey anti-rat (Jackson ImmunoResearch)). Rabbit anti-Per antiserum was diluted 1:4,000 after pre-incubation with *per*^{0} embryos. Tissues were mounted in Fluoromount-G (Southern Biotechnology) or 80% glycerol in PBS. Preparations were imaged on a Leica laser scanning confocal microscope (optical sections every 1–1.5 μm) and images were processed with Adobe Photoshop. Filter settings and laser strengths were chosen to minimize detection of green emission in the red channel in double labels. Also, for some preparations, the two channels were collected separately, using only the appropriate excitation wavelength to avoid cross-excitation. All results were qualitatively verified with single-labelling experiments.

Western blotting

Quantification of western blotting[8] was performed on scanned autoradiographs and densitometry was performed using Scion Image. Equal loading and transfer was confirmed using Ponceau-S staining of membranes.

Received 30 July; accepted 21 October 2002; doi:10.1038/nature01235.
Published online 24 November 2002.

1. Allada, R., Emery, P., Takahashi, J. S. & Rosbash, M. Stopping time: the genetics of fly and mouse circadian clocks. *Annu. Rev. Neurosci.* **24,** 1091–1119 (2001).
2. Toh, K. L. *et al.* An hPer2 phosphorylation site mutation in familial advanced sleep phase syndrome. *Science* **291,** 1040–1043 (2001).
3. Price, J. L. *et al.* double-time is a novel *Drosophila* clock gene that regulates PERIOD protein accumulation. *Cell* **94,** 83–95 (1998).
4. Kloss, B. *et al.* The *Drosophila* clock gene double-time encodes a protein closely related to human casein kinase Iε. *Cell* **94,** 97–107 (1998).
5. Martinek, S., Inonog, S., Manoukian, A. S. & Young, M. W. A role for the segment polarity gene shaggy/GSK-3 in the *Drosophila* circadian clock. *Cell* **105,** 769–779 (2001).
6. Fiol, C. J., Wang, A., Roeske, R. W. & Roach, P. J. Ordered multisite protein phosphorylation. Analysis of glycogen synthase kinase 3 action using model peptide substrates. *J. Biol. Chem.* **265,** 6061–6065 (1990).
7. Flotow, H. *et al.* Phosphate groups as substrate determinants for casein kinase I action. *J. Biol. Chem.* **265,** 14264–14269 (1990).
8. Suri, V., Hall, J. C. & Rosbash, M. Two novel doubletime mutants alter circadian properties and eliminate the delay between RNA and protein in *Drosophila*. *J. Neurosci.* **20,** 7547–7555 (2000).
9. Chen, B., Chu, T., Harms, E., Gergen, J. P. & Strickland, S. Mapping of *Drosophila* mutations using site-specific male recombination. *Genetics* **149,** 157–163 (1998).
10. Saxena, A., Padmanabha, R. & Glover, C. V. Isolation and sequencing of cDNA clones encoding alpha and beta subunits of *Drosophila melanogaster* casein kinase II. *Mol. Cell Biol.* **7,** 3409–3417 (1987).
11. Niefind, K., Guerra, B., Pinna, L. A., Issinger, O. G. & Schomburg, D. Crystal structure of the catalytic subunit of protein kinase CK2 from *Zea mays* at 2.1 ? resolution. *EMBO J.* **17,** 2451–2462 (1998).
12. Goueli, B. S., Hsiao, K., Tereba, A. & Goueli, S. A. A novel and simple method to assay the activity of individual protein kinases in a crude tissue extract. *Anal. Biochem.* **225,** 10–17 (1995).
13. Dahmus, G. K., Glover, C. V., Brutlag, D. L. & Dahmus, M. E. Similarities in structure and function of calf thymus and *Drosophila* casein kinase II. *J. Biol. Chem.* **259,** 9001–9006 (1984).
14. Helfrich-Forster, C. The period clock gene is expressed in central nervous system neurons which also produce a neuropeptide that reveals the projections of circadian pacemaker cells within the brain of *Drosophila melanogaster*. *Proc. Natl Acad. Sci. USA* **92,** 612–616 (1995).
15. Park, J. H. & Hall, J. C. Isolation and chronobiological analysis of a neuropeptide pigment-dispersing factor gene in *Drosophila melanogaster*. *J. Biol. Rhythms* **13,** 219–228 (1998).
16. Renn, S. C., Park, J. H., Rosbash, M., Hall, J. C. & Taghert, P. H. A pdf neuropeptide gene mutation and ablation of PDF neurons each cause severe abnormalities of behavioral circadian rhythms in *Drosophila*. *Cell* **99,** 791–802 (1999); erratum **101,** 113 (2000).
17. Zeng, H., Qian, Z., Myers, M. P. & Rosbash, M. A light-entrainment mechanism for the *Drosophila* circadian clock. *Nature* **380,** 129–135 (1996).
18. Harmer, S. L., Panda, S. & Kay, S. A. Molecular bases of circadian rhythms. *Annu. Rev. Cell Dev. Biol.* **17,** 215–253 (2001).
19. Sugano, S., Andronis, C., Green, R. M., Wang, Z. Y. & Tobin, E. M. Protein kinase CK2 interacts with and phosphorylates the *Arabidopsis* circadian clock-associated 1 protein. *Proc. Natl Acad. Sci. USA* **95,** 11020–11025 (1998).
20. Sugano, S., Andronis, C., Ong, M. S., Green, R. M. & Tobin, E. M. The protein kinase CK2 is involved in regulation of circadian rhythms in *Arabidopsis*. *Proc. Natl Acad. Sci. USA* **96,** 12362–12366 (1999).
21. Yang, Y., Cheng, P. & Liu, Y. Regulation of the *Neurospora* circadian clock by casein kinase II. *Genes Dev.* **16,** 994–1006 (2002).
22. Ghavidel, A. & Schultz, M. C. TATA binding protein-associated CK2 transduces DNA damage signals to the RNA polymerase III transcriptional machinery. *Cell* **106,** 575–584 (2001).
23. Keller, D. M. *et al.* A DNA damage-induced p53 serine 392 kinase complex contains CK2, hSpt16, and SSRP1. *Mol. Cell* **7,** 283–292 (2001).
24. Cashmore, A. R., Jarillo, J. A., Wu, Y. J. & Liu, D. Cryptochromes: blue light receptors for plants and animals. *Science* **284,** 760–765 (1999).
25. Allada, R., White, N. E., So, W. V., Hall, J. C. & Rosbash, M. A mutant *Drosophila* homolog of mammalian Clock disrupts circadian rhythms and transcription of period and timeless. *Cell* **93,** 791–804 (1998).
26. Hamblen, M. *et al.* Germ-line transformation involving DNA from the period locus in *Drosophila melanogaster*: overlapping genomic fragments that restore circadian and ultradian rhythmicity to per0 and per- mutants. *J. Neurogenet.* **3,** 249–291 (1986).
27. Kaneko, M., Helfrich-Forster, C. & Hall, J. C. Spatial and temporal expression of the period and timeless genes in the developing nervous system of *Drosophila*: newly identified pacemaker candidates and novel features of clock gene product cycling. *J. Neurosci.* **17,** 6745–6760 (1997).
28. Park, J. H. *et al.* Differential regulation of circadian pacemaker output by separate clock genes in *Drosophila*. *Proc. Natl Acad. Sci. USA* **97,** 3608–3613 (2000).

Acknowledgements We thank J. Rutila for assistance and guidance in conducting the genetic screen; J. Biswas for assistance with sequencing; A. McElvaine for cloning; L. McCarty for western blots; R. Scharnweber for helping to set up the CK2 activity assays; Bloomington Stock Center for fly stocks; C. Glover for CK2 antibodies; and the Northwestern University Biological Imaging Facility for assistance with confocal microscopy.

Competing interests statement The authors declare that they have no competing financial interests.

Correspondence and requests for materials should be addressed to R.A. (e-mail: r-allada@northwestern.edu).

